1999

Critical adsorption near edges

Andreas Hanke
The University of Texas Rio Grande Valley

M. Krech

F. Schlesener

S. Dietrich

Recommended Citation

Hanke, A., et al. "Critical Adsorption near Edges." Physical Review E, vol. 60, no. 5, American Physical Society, Nov. 1999, pp. 5163–74, doi:10.1103/PhysRevE.60.5163.

Critical adsorption near edges

A. Hanke,[1] M. Krech,[2] F. Schlesener,[1] and S. Dietrich[1]
[1]*Fachbereich Physik, Bergische Universität Wuppertal, D-42097 Wuppertal, Federal Republic of Germany*
[2]*Institut für Theoretische Physik, RWTH Aachen, D-52056 Aachen, Federal Republic of Germany*
(Received 14 June 1999)

Symmetry breaking surface fields give rise to nontrivial and long-ranged order parameter profiles for critical systems such as fluids, alloys, or magnets confined to wedges. We discuss the properties of the corresponding universal scaling functions of the order parameter profile and the two-point correlation function, and determine the critical exponents $\eta_{\|}$ and $\eta_{\perp}$ for the so-called normal transition. [S1063-651X(99)00411-0]

PACS number(s): 64.60.Fr, 68.35.Rh, 61.20.−p, 68.35.Bs

I. INTRODUCTION

Advanced experimental techniques have emerged which allow one to endow solid surfaces with stable geometrical structures which display a well-defined design on the scale of nanometers or micrometers. Lateral geometric structures can be formed by using various lithographic techniques such as, e.g., holographic [1], x-ray (LIGA) [2], soft [3], and nanosphere lithography [4]. These microfabrication techniques provide routes to high-quality patterns and structures with lateral dimensions down to tens of nm. These structures are either periodic in one lateral direction, consisting of grooves with various shapes of the cross section (e.g., wedgelike), or they display periodicity in both lateral dimensions.

These manmade surfaces offer a wide range of possible applications if they are exposed to fluids. In that case the surfaces act as a template with a designed topography which imposes specified lateral structures on a fluid. For example, in the context of microfluidics [5,6] these geometrical structures can be used as guiding systems in order to deliver tiny amounts of valuable liquids to designated analysis centers on a solid surface as part of microscopic chemical factories [7]. Besides the numerous experimental challenges associated with these systems, there is also the theoretical challenge to understand the corresponding highly inhomogeneous fluid structures (and ultimately the flow dynamics) as well as to guide the design on the basis of this insight [8].

In view of this goal the study of the fluid structures in a single wedgelike groove with opening angle α serves as a paradigmatic first step. For $\alpha=\pi$ the geometry reduces to the well-studied case of a planar substrate. For decreasing values of α the fluid is squeezed, whereas for $\alpha>\pi$ a ridgelike solid perturbation is projected into the fluid. Due to the unbound accessible space for all values of α, the bulk properties of the fluid are unchanged by the presence of the wedge. (This is an important difference as compared with pores in which the confinement alters the bulk properties.) At low temperatures one finds pronounced packing effects for the fluid particles near the corner of the wedge which differ significantly from those encountered at planar surfaces [9–11]. Even stronger effects occur if the wedge is exposed to a vapor phase. In this case a liquidlike meniscus is formed at the bottom of the wedge which undergoes a filling transition at a temperature T_{α} *below* the wetting transition temperature T_W of the corresponding planar substrate [12–15]. It has been demonstrated that x-ray scattering experiments at grazing incidence are capable of resolving such interfacial structures [16,17].

If the temperature is increased sufficiently above the triple point of the fluid one encounters its bulk critical point T_c. This can be either the liquid-vapor critical point of the fluid or the demixing critical point if the fluid is a binary liquid mixture. The experience with planar surfaces tells [18,19] that at bulk criticality the confinement triggers interesting new surface critical phenomena. In this case the local order parameter ϕ is perturbed near the surface within a layer whose thickness is governed by the diverging bulk correlation length $\xi_{\pm}(t\to 0)=\xi_0^{\pm}|t|^{-\nu}$, where $t=(T-T_c)/T_c$; ν denotes the universal bulk critical exponent and $\xi_0^{\pm}$ is the nonuniversal amplitude above $(+)$ and below $(-)T_c$. Thus at T_c the perturbation due to the surface intrudes deeply into the bulk.

In order to extend our knowledge of the structure of confined fluids to these elevated temperatures, we set out to investigate the aforementioned surface critical phenomena in a wedge. Based on analytic calculations [20–27] and computer simulations [28,29], the local critical behavior in a wedge has been analyzed for the case that the corresponding planar surface exhibits the so-called *ordinary* or *special* surface phase transitions [18,19]. In the corresponding magnetic language the ordinary phase transition corresponds to the case that the couplings between the surface spins remain below the threshold value of the multicritical special transition beyond which the surface can support long-ranged order even above T_c [18,19], and in which there are no surface fields. The ordinary transition has also been studied for different shapes of the confinement such as parabolic ones [30–32]. The main concern of these studies has been critical edge exponents describing the leading critical behavior of the order parameter near the corner, which differs from that at planar surfaces and in the bulk. One finds that in general the edge exponents depend on the opening angle α. These studies aim at describing magnetic systems in the absence of surface fields, as they are experimentally accessible, e.g., by scanning electron microscopy [33].

However, the aforementioned surface and edge universality classes are not applicable in the present context of confined fluids. For example, in a binary liquid mixture one of the two species will prefer the confining substrate more than the other, which results in an effective surface field acting on the order parameter given by the concentration

difference between the two species. Similar arguments hold for a one-component fluid near liquid-vapor coexistence. These surface fields give rise to another surface universality class, the so-called *normal* transition [18,19]. This differs from the ordinary and special transitions discussed above in that these symmetry breaking surface fields generate a nontrivial order parameter profile even if the bulk is in the disordered phase, i.e., for $T \geqslant T_c$. For a planar surface this gives rise to the well-studied so-called *critical adsorption* phenomenon (see, e.g., Refs. [18,19,34–38]). Here we extend the corresponding field-theoretical analysis for the normal transition to the wedge geometry under consideration. After presenting our model and discussing general scaling properties (Sec. II) we analyze the order parameter profile in Sec. III and the structure factor in Sec. IV. By focusing on the critical temperature $T = T_c$ we are able to obtain analytical results. They are summarized in Sec. V. Appendixes A and B contain important technical details needed in Secs. III and IV.

Experimentally, wedges are characterized by a finite depth Λ. Moreover, in many cases they are manufactured as a laterally periodic array of parallel grooves and ridges. The structural properties of a fluid exposed to such a periodic array depend sensitively on the ratio Λ/ξ of the depth and the correlation length. For $\Lambda/\xi \ll 1$ the system will resemble a critical fluid exposed to a mildly corrugated substrate, which is expected to give rise to corrections to the leading critical adsorption behavior at a planar substrate. For $\Lambda/\xi \gg 1$ near the tip of a ridge and near the bottom of a groove the presence of their periodic duplicates becomes irrelevant, so that in this limit the edge singularity of a single edge with $\alpha > \pi$ and $\alpha < \pi$, respectively, will prevail. Our present study deals with the limit $\Lambda \to \infty$ and $\xi \to \infty$ taken such that $\Lambda/\xi \gg 1$. Certainly, in a later stage it will be rather rewarding also to study the crossover regime $\Lambda/\xi \approx 1$ in which the grooves and the ridges as well as the way they are joined together play an equally important role. The occurrence of the unbending transition in the case of wetting on corrugated substrates [39] indicates that the regime $\Lambda/\xi \approx 1$ might exhibit rather interesting new phenomena.

II. MODEL AND GENERAL RESULTS

Our investigation is based on the Ginzburg-Landau Hamiltonian $\mathcal{H}$ determining the statistical weight $\exp(-\mathcal{H})$ for a scalar order parameter ϕ which represents a critical system within the Ising universality class. According to the wedge geometry, $\mathcal{H}$ is given as a sum of three contributions, i.e., $\mathcal{H} = \mathcal{H}_b + \mathcal{H}_s + \mathcal{H}_e$, which refer to the bulk (b), the surface (s), and the edge (e) contributions, respectively. In cylindrical coordinates $\mathbf{r} = (r, \theta, \mathbf{x}_\parallel)$ (see Fig. 1), the individual contributions are given by

$$\mathcal{H}_b[\phi] = \int_0^\alpha d\theta \int_0^\infty dr\, r \int d^{d-2}x_\parallel \left\{ \frac{1}{2}(\nabla\phi)^2 + \frac{\tau}{2}\phi^2 + \frac{g}{4!}\phi^4 \right\}, \tag{2.1a}$$

$$\mathcal{H}_s[\phi] = \int_0^\infty dr \int d^{d-2}x_\parallel \left\{ \frac{c_1}{2}[\phi(r,0,\mathbf{x}_\parallel)]^2 - h_1\phi(r,0,\mathbf{x}_\parallel) + \frac{c_2}{2}[\phi(r,\alpha,\mathbf{x}_\parallel)]^2 - h_2\phi(r,\alpha,\mathbf{x}_\parallel) \right\}, \tag{2.1b}$$

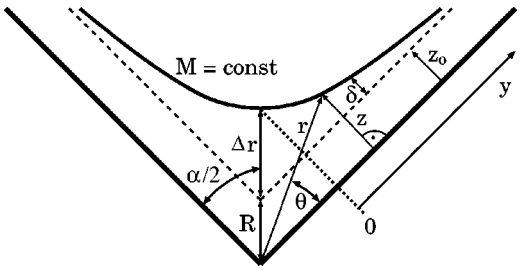

FIG. 1. Cross section of a wedge perpendicular to its edge with opening angle α. The system is translationally invariant in the $(d-2)$-dimensional subspace parallel to the edge. The curve labeled ''$M = \text{const}$'' represents a contour line of the order parameter profile (see Sec. III B). r and $0 \leqslant \theta \leqslant \alpha$ are cylindrical coordinates. $z = r \sin\theta$ is the normal distance from the surface of the wedge. The dashed lines are the asymptotes of the contour line $M = \text{const}$ which are a distance z_0 apart from the surface. $R = z_0/\sin(\alpha/2)$ is the distance between the intersection of the asymptotes and the edge of the wedge. $\Delta r + R$ is the distance between the contour line in the center and the edge. The contour line approaches the asymptotes such that $\delta(y \to \infty) \to 0$ and $\delta(y = 0) = \Delta r \sin(\alpha/2)$, where y measures the distance along the wall.

$$\mathcal{H}_e[\phi] = \int d^{d-2}x_\parallel \left\{ \frac{c_e}{2}[\phi(0,0,\mathbf{x}_\parallel)]^2 - h_e\phi(0,0,\mathbf{x}_\parallel) \right\}, \tag{2.1c}$$

where d is the space dimension and $\mathbf{x}_\parallel$ parametrizes the $(d-2)$-dimensional subspace parallel to the edge along which the system is translationally invariant. The bulk Hamiltonian $\mathcal{H}_b$ given by Eq. (2.1a) represents the standard Ginzburg-Landau ϕ^4 model in the absence of external bulk fields. The bulk parameter τ is proportional to the reduced temperature $t = (T - T_c)/T_c$, g is the bulk coupling constant, and α denotes the opening angle. The surface Hamiltonian $\mathcal{H}_s$ given by Eq. (2.1b) captures the effect of the two semi-infinite planar surfaces forming the geometric boundaries of the wedge located at $\theta = 0$ and $\theta = \alpha$, respectively. Note that $\mathcal{H}_b$ and $\mathcal{H}_s$ take their standard fixed-point form with a surface enhancement c_i and a surface field h_i for each of the surfaces $i = 1$ and 2. Cubic surface fields [34] will be disregarded here. The surfaces meet at the opening angle α along the edge of the wedge which gives rise to the third contribution $\mathcal{H}_e$. The edge Hamiltonian $\mathcal{H}_e$ given by Eq. (2.1c) has the same structure as the surface contribution $\mathcal{H}_s$, and is characterized by an edge enhancement c_e and an edge field h_e [19]. The total Hamiltonian $\mathcal{H}$ constitutes a renormalizable model (see Sec. IV A 3 in Ref. [19]).

In this investigation we are exclusively concerned with the normal transition which is characterized by nonzero values of all surface and edge fields h_1, h_2, and h_e and arbitrary values of the surface enhancements c_1 and c_2 and of the edge enhancement c_e. For nonzero fields h_1 or h_2 the system is *ordered* at any finite point even for $T > T_c$. Asymptotically close to the critical point T_c, the universal properties of the corresponding order parameter profile are linked to the *critical adsorption fixed point* of the corresponding renormalization group description. The ensuing scaling functions refer to the scaling limits $r \to \infty$ and $\xi \to \infty$, where the ratio r/ξ is kept fixed forming a finite scaling variable. *At* the critical

adsorption fixed point the surface fields are infinitely large, so that the order parameter profile

$$M(r,\theta,t;\alpha)\equiv\langle\phi(r,\theta,\mathbf{x}_\parallel)\rangle \tag{2.2}$$

diverges at the surfaces $\theta=0$ and $\theta=\alpha$ of the wedge according to a power law. (We recall that such divergences refer to the renormalization group fixed point, whereas actually the divergence of the order parameter profile is cut off at atomic distances from the surfaces.) Consequently, at this so-called normal transition the surfaces can differ at most with respect to the sign of the fields. In the following we assume that the surface fields have the same sign, and we denote this configuration as $(+,+)$. Note that only $\mathcal{H}_b$ in conjunction with the aforementioned boundary conditions is left to determine the functional form of the order parameter profile.

Close to the critical point T_c, the order parameter profile takes the scaling form

$$M(r,\theta,t;\alpha)=a|t|^{\beta}P_{\pm}(r/\xi_{\pm},\theta;\alpha), \tag{2.3}$$

where $\xi_{\pm}=\xi_0^{\pm}|t|^{-\nu}$ with $t=(T-T_c)/T_c\gtrless 0$ is the correlation length, and $P_{\pm}(\zeta_{\pm},\theta;\alpha)$ are the corresponding scaling functions with the scaling variable

$$\zeta_{\pm}=r/\xi_{\pm}. \tag{2.4}$$

The amplitude a in Eq. (2.3) is the nonuniversal amplitude of the bulk order parameter $M_b=a|t|^{\beta}$, $T<T_c$, where β is the corresponding bulk critical exponent. The scaling functions $P_{\pm}$ are universal and have the limiting behaviors $P_+(\zeta_+\to\infty,\theta;\alpha)\to 0$ and $P_-(\zeta_-\to\infty,\theta;\alpha)\to 1$, respectively. Note that P_+ and P_- are universal but depend on the *definition* of the correlation length $\xi_{\pm}$, because $\xi_{\pm}$ enters the scaling argument $\zeta_{\pm}$. In the opposite limit $\zeta_{\pm}\to 0$, i.e., $T\to T_c$, the scaling functions $P_{\pm}$ exhibit short-distance singularities in form of power laws which reflect the anomalous scaling dimension of the order parameter ϕ:

$$P_{\pm}(\zeta_{\pm}\to 0,\theta;\alpha)=\tilde{\mathcal{C}}_{\pm}(\theta;\alpha)\zeta_{\pm}^{-\beta/\nu}. \tag{2.5}$$

The ratio β/ν of critical exponents has the values 1 in $d=4$, $\simeq 0.5168$ in $d=3$ [40], and 1/8 in $d=2$. Equation (2.5) implies a power law dependence on r for the order parameter profile at criticality:

$$M(r,\theta,t=0;\alpha)=a\tilde{\mathcal{C}}_{\pm}(\theta;\alpha)(r/\xi_0^{\pm})^{-\beta/\nu}. \tag{2.6}$$

The scaling functions $\tilde{\mathcal{C}}_{\pm}(\theta;\alpha)$ appearing in Eqs. (2.5) and (2.6) are universal but depend on the definition of the correlation length because they are derived from $P_{\pm}$. [However, the product $\tilde{\mathcal{C}}_{\pm}(\xi_0^{\pm})^{\beta/\nu}$ is invariant with respect to different choices for the definition of the bulk correlation length.] In order to be specific we choose as the definition for ξ the so-called *true* correlation length which governs the decay of the two-point correlation function in the bulk system [37]. Equation (2.6) implies the relation

$$\tilde{\mathcal{C}}_+(\theta;\alpha)/\tilde{\mathcal{C}}_-(\theta;\alpha)=(\xi_0^+/\xi_0^-)^{-\beta/\nu} \tag{2.7}$$

between the scaling functions $\tilde{\mathcal{C}}_{\pm}$ involving the universal ratio ξ_0^+/ξ_0^-.

In the limit $\alpha=\pi$ the wedge geometry coincides with the semi-infinite geometry. In this limit the universal scaling functions $\tilde{\mathcal{C}}_{\pm}$ reduce to

$$\tilde{\mathcal{C}}_{\pm}(\theta;\alpha=\pi)=c_{\pm}(\sin\theta)^{-\beta/\nu}, \tag{2.8}$$

where the universal amplitudes $c_{\pm}$ with $c_+/c_-=(\xi_0^+/\xi_0^-)^{-\beta/\nu}$ govern the critical adsorption profile at a planar surface [37], so that

$$\begin{aligned}M(r,\theta,t=0;\alpha=\pi)&=M_{\infty/2}(z=r\sin\theta,t=0)\\&=ac_{\pm}(z/\xi_0^{\pm})^{-\beta/\nu}\end{aligned} \tag{2.9}$$

yields the order parameter profile $M_{\infty/2}$ in the semi-infinite system at criticality. The profile $M_{\infty/2}(z_0,t=0)$ at a reference distance z_0 from the surface can be used in order to construct the ratio

$$\frac{M(r,\theta,t=0;\alpha)}{M_{\infty/2}(z_0,t=0)}=\mathcal{C}(\theta;\alpha)\rho^{-\beta/\nu},\quad \rho=r/z_0, \tag{2.10}$$

which is independent of the nonuniversal amplitudes a and $\xi_0^{\pm}$. Here we have introduced the length ratio $\rho=r/z_0$ and the scaling function

$$\mathcal{C}(\theta;\alpha)\equiv\tilde{\mathcal{C}}_+(\theta;\alpha)/c_+=\tilde{\mathcal{C}}_-(\theta;\alpha)/c_-. \tag{2.11}$$

We note that $\mathcal{C}$ is not only universal but also independent of the definition for the correlation length, because the left-hand side of Eq. (2.10) and ρ are expressed in terms of order parameter profiles and distances, respectively, without resorting to the notion of the correlation length.

In the limit that the normal distance $z=r\sin\theta$ from the surface of the wedge is much smaller than r, i.e., for $\theta\to 0$ with r fixed, the order parameter profile reduces to the planar semi-infinite behavior

$$\begin{aligned}M(r,\theta,t=0;\alpha)&=ac_{\pm}(z/\xi_0^{\pm})^{-\beta/\nu}\\&\to ac_{\pm}\theta^{-\beta/\nu}(r/\xi_0^{\pm})^{-\beta/\nu},\quad \theta\to 0,\end{aligned} \tag{2.12}$$

so that Eqs. (2.9) and (2.10) imply

$$\mathcal{C}(\theta\to 0;\alpha)\to\theta^{-\beta/\nu},\qquad \mathcal{C}(\theta\to\alpha;\alpha)\to(\alpha-\theta)^{-\beta/\nu}, \tag{2.13}$$

where we have used the symmetry property

$$\mathcal{C}(\theta;\alpha)=\mathcal{C}(\alpha-\theta;\alpha). \tag{2.14}$$

III. ORDER PARAMETER PROFILE AT T_c

At the critical point the radial dependence of the order parameter profile in the wedge is given by the power law $r^{-\beta/\nu}$ [see Eq. (2.6)]. The dependence of the profile on θ is captured by the universal amplitude function $\mathcal{C}(\theta;\alpha)$ [see Eq. (2.10)], which in $d=2$ is determined by conformal invariance arguments (see Sec. III D). In $d>2$, however, one has to resort to explicit field-theoretical calculations, assuming that the amplitude function $\mathcal{C}$, as other universal quantities, is a smooth function of the spatial dimension d. In the

following we focus on the corresponding mean-field description, i.e., lowest order perturbation theory within the field-theoretical approach. The mean-field results become exact at the upper critical dimension $d_{uc}=4$ of the field theory described by Eq. (2.1), i.e., for $d\nearrow 4$. In order to provide an estimate for the order parameter profile in $d=3$ we shall use the exact results in $d=2$ and the mean-field results in $d=4$ for an interpolation scheme between $d=2$ and 4, where the correct scaling arguments and short-distance singularities are implemented. For the order parameter profile studied here we shall use the value $\beta/\nu\simeq 0.5168$ [40] in $d=3$ instead of the mean-field value $\beta/\nu=1$. Thus only the amplitude function is treated in lowest order perturbation theory.

A. Mean-field theory

Within mean-field theory it is convenient to introduce the reduced profile

$$m(r,\theta,\tau;\alpha)\equiv\sqrt{g/12}M(r,\theta,\tau;\alpha); \tag{3.1}$$

$m(r,\theta,\tau;\alpha)$ is determined by the Euler-Lagrange equation

$$\left[\frac{\partial^2}{\partial r^2}+\frac{1}{r}\frac{\partial}{\partial r}+\frac{1}{r^2}\frac{\partial^2}{\partial\theta^2}\right]m=\tau m+2m^3 \tag{3.2}$$

for $r>0$ and $0<\theta<\alpha$. The divergences of the profile m near the surfaces and the edge of the wedge account for the effect of the surface and edge parts of the Hamiltonian in the $(+,+)$ configuration considered here. For $\tau=0$, Eq. (3.2) implies, for the universal amplitude function

$$\mathcal{C}(\theta;\alpha)=rm(r,\theta,\tau=0;\alpha), \tag{3.3}$$

[see Eq. (2.10), here $\beta/\nu=1$] the equation

$$\frac{\partial^2}{\partial\theta^2}\mathcal{C}(\theta;\alpha)=-\mathcal{C}(\theta;\alpha)+2[\mathcal{C}(\theta;\alpha)]^3. \tag{3.4}$$

Equation (3.4) leads to exact results for $\mathcal{C}$ in the limit $d\nearrow 4$. Note that Eq. (3.4) can readily be solved using the order parameter profile obtained for a *film geometry* with $(+,+)$ boundary conditions [41]. Specifically, Eq. (3.4) is equivalent to the Euler-Lagrange equation for a film with thickness L as given by Eq. (A3) in Ref. [41] if the rescaled temperature τL^2 there is replaced by $-\alpha^2$. The expression θ/α for the wedge corresponds to z/L for the film. The solution of Eq. (3.4) can be expressed by the Jacobian elliptic functions sn and dn,

$$\mathcal{C}(\theta;\alpha)=\frac{1}{\sqrt{1-2k^2(\alpha)}}\frac{\mathrm{dn}(\theta/\sqrt{1-2k^2(\alpha)};k(\alpha))}{\mathrm{sn}(\theta/\sqrt{1-2k^2(\alpha)};k(\alpha))},$$

$$0\leqslant\alpha\leqslant\pi, \tag{3.5a}$$

in terms of the modulus k of the complete elliptic integral $K(k)$ of the first kind (see Appendix A), where $k=k(\alpha)$ is implicitly given by

$$\alpha=2K(k)\sqrt{1-2k^2},\quad 1/2\geqslant k^2\geqslant 0, \tag{3.5b}$$

[see Eqs. (A12) and (A13) in Ref. [41]] and

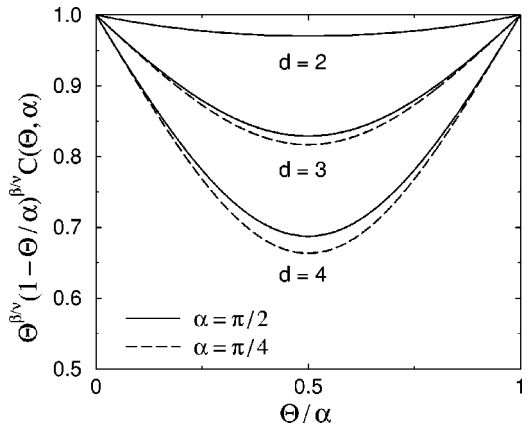

FIG. 2. Universal scaling function $\mathcal{C}(\theta;\alpha)$ [see Eq. (2.10)] as function of the polar angle θ for fixed opening angles $\alpha=\pi/2$ and $\alpha=\pi/4$ (compare Fig. 1). The divergences at $\theta=0$ and $\theta=\alpha$ are split off [compare Eq. (2.13)]. The curves for $d=3$ show the linear interpolation between the corresponding exactly known curves for $d=2$ [see Eq. (3.24)] and $d=4$ [see Eq. (3.5)]. Note that the shape of the curve for $d=2$ is independent of α for $0<\alpha<\pi$.

$$\mathcal{C}(\theta;\alpha)=\frac{1}{\sqrt{1+k^2(\alpha)}}\frac{1}{\mathrm{sn}(\theta/\sqrt{1+k^2(\alpha)};k(\alpha))},$$

$$\pi\leqslant\alpha\leqslant 2\pi, \tag{3.6a}$$

where now $k=k(\alpha)$ is implicitly given by

$$\alpha=2K(k)\sqrt{1+k^2},\quad 0\leqslant k\leqslant k_{\max}\simeq 0.90953 \tag{3.6b}$$

[see Eqs. (A14) and (A15) in Ref. [41]]. In the following we consider only the case $0\leqslant\alpha\leqslant\pi$; according to Eq. (3.6), the extension to the case $\pi\leqslant\alpha\leqslant 2\pi$ is straightforward. Note that the parametrizations of the opening angle α as given by Eqs. (3.5b) and (3.6b) are monotonous functions of the modulus k, and therefore the inverse function $k(\alpha)$ is uniquely defined but cannot be expressed in closed form in general. The special case $\alpha=\pi$ corresponds to $k(\alpha=\pi)=0$ so that $\mathcal{C}(\theta;\alpha=\pi)=1/\sin\theta$, which reproduces the mean-field result for the order parameter profile in the semi-infinite geometry at the normal transition expressed in polar coordinates [see Eqs. (2.8) and (2.11); here $\beta/\nu=1$]. The shape of $\mathcal{C}(\theta;\alpha)$ for $d=2$ [see Eq. (3.24) in Sec. III D] and $d=4$ [see Eq. (3.5)] for fixed opening angles $\alpha=\pi/2$ and $\pi/4$ is shown in Fig. 2, where the divergences at $\theta=0$ and $\theta=\alpha$ according to Eq. (2.13) have been split off. As an estimate for $d=3$, in Fig. 2 we show the linear interpolation between the corresponding curves for $d=2$ and 4.

B. Contour lines of the order parameter profile

One of the motivations for our investigation of criticality in the wedge geometry is the frequent use of grooved substrates as templates to impose inhomogeneous structures on liquids. In the wedge geometry the density (or concentration) of the adsorbed critical fluid is inhomogeneous within planes perpendicular to the edge. The intersection of these planes with surfaces of constant order parameter $M(r,\theta,t=0;\alpha)=M_0$ renders the contour lines $r=r(\theta;\alpha,M_0)$ of the order parameter profile, which characterize the inhomogeneous

shape of the order parameter configuration in the wedge. Far away from the center of the wedge the order parameter profile approaches the profile for a planar substrate so that the contour lines asymptotically become straight lines parallel to the surfaces forming the wedge (compare Fig. 1). As expected, the deviation of the contour lines from these parallel straight lines is largest in the center of the wedge. The normalized order parameter profile defined by the left-hand side of Eq. (2.10) yields the contour lines

$$\frac{r(\theta,\alpha)}{z_0}=[\mathcal{C}(\theta;\alpha)]^{\nu/\beta}, \tag{3.7}$$

where for a given contour line the reference distance z_0 is fixed by the asymptotic distance of this contour line from the wedge surface, i.e., by $M_0=M_{\infty/2}(z_0,t=0)$ (see Fig. 1). Thus the angular dependence of *every* contour line exhibits the *same* universal shape in units of the corresponding asymptotic distance z_0. Equations (2.13) and (3.7) imply that $r(\theta\to 0,\alpha)\sim\theta^{-1}$ independent of d and α.

Within mean-field theory (for which $\beta/\nu=1$) we obtain from Eq. (3.5) in the center of the wedge, i.e., for $\theta=\alpha/2$,

$$\frac{r(\theta=\alpha/2,\alpha)}{z_0}=\mathcal{C}(\theta=\alpha/2;\alpha)=\frac{\sqrt{1-k^2(\alpha)}}{\sqrt{1-2k^2(\alpha)}},\quad d=4. \tag{3.8}$$

According to Fig. 1 the distance R of the intersection of the asymptotes from the edge is given by $R=z_0/\sin(\alpha/2)$ which implies for the deviation $\Delta r=r-R$ of the contour line at the center of the wedge:

$$\Delta r=\left[\frac{\sqrt{1-k^2(\alpha)}}{\sqrt{1-2k^2(\alpha)}}-\frac{1}{\sin(\alpha/2)}\right]z_0,\quad d=4. \tag{3.9}$$

In order to discuss Eq. (3.9), we first consider a very wide wedge, i.e., the limit $\alpha\to\pi$ for which $k^2\to 0$. In this limit the deviation Δr decays according to [see Eqs. (3.5b) and (A2)]

$$\frac{\Delta r}{z_0}=\frac{2}{3}\left(1-\frac{\alpha}{\pi}\right)+\left(\frac{5}{6}-\frac{\pi^2}{8}\right)\left(1-\frac{\alpha}{\pi}\right)^2+O\left(\left(1-\frac{\alpha}{\pi}\right)^3\right),\quad d=4. \tag{3.10}$$

In the opposite limit of a very narrow wedge, i.e., for $\alpha\to 0$, the deviation Δr of the contour line in the center *diverges* according to

$$\frac{\Delta r}{z_0}=\frac{\Omega}{\alpha}+O(\alpha),\quad d=4, \tag{3.11}$$

where $\Omega=\sqrt{2}K(1/\sqrt{2})-2\simeq 0.622$. This shows that the contour lines are expelled from the wedge into the bulk for small opening angles. The overall behavior of Δr for $0\leqslant\alpha\leqslant\pi$ for $d=2$ [see Eq. (3.26) in Sec. III D] and $d=4$ [see Eq. (3.9)] is shown in Fig. 3. Again, the curve for $d=3$ represents the estimate obtained by the linear interpolation between the curves for $d=2$ and 4 (compare Fig. 2).

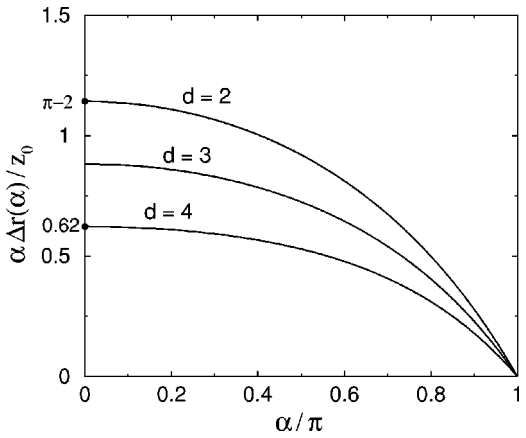

FIG. 3. Universal dependence of the deviation $\Delta r=r-R$ in units of the reference distance z_0 of the contour line at the center of the wedge (compare Fig. 1) on the opening angle α. The curve for $d=3$ shows the linear interpolation between the exactly known curves for $d=2$ [see Eq. (3.26)] and $d=4$ [see Eq. (3.9)]. Δr is multiplied by α so that the product $\alpha\Delta r$ attains a finite value for $\alpha\to 0$ [see Eq. (3.28) for $d=2$ and Eq. (3.11) for $d=4$; we assume in addition that the power law $\Delta r(\alpha\to 0)\sim\alpha^{-1}$ remains valid for $2<d<4$].

C. Distant wall corrections

Far away from the center of the wedge the contour lines of the order parameter profile approach straight lines which are parallel to the wedge surfaces (compare Fig. 1). This implies that in this limit the deviation of the order parameter profile from the corresponding profile in a semi-infinite geometry becomes small. This small deviation can be interpreted in terms of the so-called distant-wall correction which is obtained from the *short-distance expansion* [42–46] of the order parameter near, say, the surface $\theta=0$ of the wedge. For any scaling operator Ψ the short-distance expansion at the normal transition can be written as

$$\Psi(r,\theta,\mathbf{x}_\parallel)=\langle\Psi(r,\theta,\mathbf{x}_\parallel)\rangle_{\infty/2}[1+b_\Psi T_{\theta\theta}(r,0,\mathbf{x}_\parallel)(r\theta)^d+O(\theta^{d+2})], \tag{3.12}$$

where $T_{\theta\theta}=T_{\perp\perp}$ denotes the stress tensor component *perpendicular* to the wall at $\theta=0$ and $r\theta\ll r\alpha$ is the small distance from the wall. For the order parameter profile $M=\langle\phi\rangle$ from Eq. (3.12) we infer

$$M(r,\theta;\alpha)=M(r,\theta;\pi)[1+B_\phi\theta^d+\cdots], \tag{3.13}$$

in analogy to the short-distance expansion of the order parameter profile in the film geometry [47], where $B_\phi=b_\phi\langle T_{\theta\theta}\rangle r^d$. From the general expression of the stress tensor at criticality [see Eq. (3.1) in Ref. [46]], in polar coordinates we obtain

$$T_{\theta\theta}=\frac{1}{2r^2}\left(\frac{\partial\phi}{\partial\theta}\right)^2-\frac{1}{2}\left(\frac{\partial\phi}{\partial r}\right)^2-\frac{1}{2}(\nabla_\parallel\phi)^2-\frac{g}{24}\phi^4+\frac{d-2}{4(d-1)}\left[\frac{\partial^2}{\partial r^2}\phi^2+\Delta_\parallel\phi^2\right] \tag{3.14}$$

up to contributions of the order g^3, where $\nabla_\parallel$ and $\Delta_\parallel$ denote the components of the gradient and the Laplacian along the edge, respectively.

Within mean-field theory the thermal average of Eq. (3.14) is obtained by setting $d=4$ and replacing ϕ by $\langle\phi\rangle = \sqrt{12/g}\ m$ [see Eqs. (3.1) and (3.3)]. Since the result is independent of θ we can use the fact that the order parameter profile is symmetric around the midplane $\theta=\alpha/2$ in order to obtain

$$\langle T_{\theta\theta}\rangle = \frac{6}{gr^4}[[\mathcal{C}(\alpha/2;\alpha)]^2 - [\mathcal{C}(\alpha/2;\alpha)]^4], \quad d=4. \tag{3.15}$$

From Eq. (3.5) we thus find

$$\langle T_{\theta\theta}\rangle = -\frac{6}{gr^4}\frac{k^2(\alpha)[1-k^2(\alpha)]}{[1-2k^2(\alpha)]^2}, \quad d=4, \tag{3.16}$$

which exactly corresponds to $\langle T_{zz}\rangle$ in the film geometry with $(+,+)$ boundary conditions [see the first line of Eq. (3.4) in Ref. [41] for $y=-1$]. If Eq. (3.16) is inserted into Eq. (3.12) for $\Psi=\phi$ the structure of the distant-wall correction as given by Eq. (3.13) is confirmed. However, for a complete identification the amplitude b_ϕ must be determined. Within the present mean-field approach Eq. (3.13) can directly be verified by expanding Eq. (3.5) for $\theta\to 0$ with α fixed. From the expansions of the Jacobian elliptic functions [see Eq. (A6)] we obtain

$$m(r,\theta;\alpha) = m(r,\theta;\pi)\left[1+\frac{k^2(\alpha)[1-k^2(\alpha)]}{[1-2k^2(\alpha)]^2}\left(\frac{\theta^4}{10}-\frac{\theta^6}{105}\right) + O(\theta^8)\right], \quad d=4, \tag{3.17}$$

from which one can read off $b_\phi=-g/60$ within mean-field theory. The next-to-leading correction $O(\theta^6)$ in Eq. (3.17) is generated by the operator $\Delta_r T_{\theta\theta}$ where Δ_r denotes the radial part of the Laplacian in polar coordinates $(r,\theta,\mathbf{x}_\parallel)$. In general the corresponding correction is $O(\theta^{d+2})$ as indicated in Eq. (3.12). In principle $\Delta_\parallel T_{\theta\theta}$ also yields a contribution to the short-distance expansion, but one has $\Delta_\parallel\langle T_{\theta\theta}\rangle=0$ due to the translational invariance along the $(d-2)$-dimensional edge. We note that in the *film geometry* the counterpart of the operator $\Delta_r T_{\theta\theta}$ in the wedge does *not* contribute to the next-to-leading distant-wall correction of the order parameter profile due to the translational invariance in the film. Therefore in the film the next-to-leading correction is given by the operator $(T_{\perp\perp})^2$, which gives rise to $O(\theta^{2d})$ corrections only. The latter operator also appears in the wedge geometry and gives rise to the $O(\theta^8)$ corrections indicated in Eq. (3.17).

The distant-wall correction has an interesting geometric interpretation. The contour lines of the order parameter profile in the wedge and in the semi-infinite geometry, respectively, belonging to the same value M_0 of the order parameter, are displaced by an amount $\delta(y;\alpha)$ where $\delta+z_0=z=r\sin\theta$ and the distance y is related to θ by (compare Fig. 1)

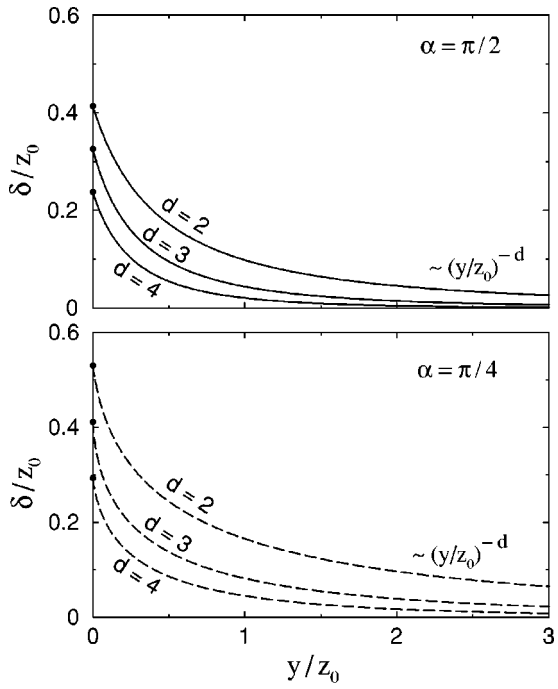

FIG. 4. Universal dependence of the displacement $\delta(y;\alpha)$ of the contour line from its asymptote on the distance y [compare Fig. 1, and see Eqs. (3.20) and (3.18)] for fixed opening angles $\alpha=\pi/2$ and $\pi/4$. The curves for $d=3$ correspond to a suitable interpolation [see Eq. (3.22)] between the exactly known curves for $d=2$ and 4, so that for $y/z_0\to\infty$ they exhibit the correct asymptotic decay $\sim(y/z_0)^{-3}$ in accordance with the distant-wall correction.

$$y = y(\theta,\alpha) = r(\theta,\alpha)\cos\theta - [R(\alpha)+\Delta r(\alpha)]\cos(\alpha/2). \tag{3.18}$$

Within mean-field theory, for the above choice of M_0 [see Eq. (3.7), here $\beta/\nu=1$] and using $r/z_0=\mathcal{C}(\theta;\alpha)$, one obtains

$$\frac{\delta(y(\theta,\alpha);\alpha)}{z_0} = \mathcal{C}(\theta;\alpha)\sin(\theta) - 1 = \frac{m(r,\theta;\alpha)}{m(r,\theta;\pi)} - 1, \quad d=4. \tag{3.19}$$

According to Eqs. (3.13) and (3.19) the ratio $\delta(y(\theta,\alpha);\alpha)/z_0$ as a function of θ represents the distant-wall correction of the order parameter profile. Its leading terms can be read off from Eq. (3.17). For general d one has [see Eq. (3.7)]

$$\frac{\delta(y(\theta,\alpha);\alpha)}{z_0} = [\mathcal{C}(\theta,\alpha)]^{\nu/\beta}\sin(\theta) - 1, \tag{3.20}$$

so that $\delta/z_0\to(1/6)[(\pi/\alpha)^2-1]\theta^2$ for $d=2$ and $\theta\to 0$ [see Eq. (3.24) in Sec. III D]. The behavior of $\delta(y,\alpha)$ as function of y for fixed opening angles $\alpha=\pi/2$ and $\pi/4$ is shown in Fig. 4 for $d=2$ [see Eq. (3.24)] and $d=4$ [see Eq. (3.19)]. In order to obtain an estimate for $d=3$, we introduce

$$f(\theta;\alpha) = \frac{\delta(y(\theta,\alpha);\alpha)}{z_0}\left(\frac{2\theta}{\alpha}\right)^{-d}. \tag{3.21}$$

One has $\delta/z_0\sim\theta^d$ for $\theta\to 0$ or $\sim y^{-d}$ for $y\to\infty$ due to $y(\theta\to 0,\alpha)\sim r(\theta\to 0,\alpha)\sim\theta^{-1}$ [see Eq. (3.18)]. Therefore

$f(\theta;\alpha)$ tends for $\theta\to 0$ to a constant value (depending on d). For $y=0$ one has $2\theta/\alpha=1$ and $f=\Delta r\sin(\alpha/2)/z_0$ (compare Figs. 1 and 3). A reasonable estimate for $\delta(y;\alpha)$ in $d=3$ can be obtained by interpolating $f(\theta;\alpha)$ linearly between $d=2$ and 4 and using this approximation for f in

$$\frac{\delta(y(\theta,\alpha);\alpha)}{z_0}=f(\theta;\alpha)\left(\frac{2\theta}{\alpha}\right)^3, \quad d=3. \tag{3.22}$$

The curves for $d=3$ in Fig. 4 correspond to the right-hand side of Eq. (3.22) for fixed values $\alpha=\pi/2$ and $\pi/4$. For $y=0$ one has $2\theta/\alpha=1$, so that for $y=0$ the linear interpolation of f implies a linear interpolation of δ [see Eq. (3.21)].

D. Exact results in $d=2$

At criticality systems exhibit not only scale invariance but, more generally, *conformal* invariance [44]. This property is particularly useful in $d=2$, where the *large conformal group* provides mappings between many different geometries [44]. In higher spatial dimensions only Möbius transformations are available as conformal mappings (small conformal group) which map geometries bounded by planes and spheres onto other geometries bounded by planes and spheres. In $d=2$ a wedge with opening angle α can be conformally mapped onto a half-plane, for which the profile is known. This leads to [48]

$$M(r,\theta,t=0;\alpha)\equiv\langle\phi\rangle_{\text{wedge}}=A(\pi/\alpha)^{\beta/\nu}[r\sin(\theta\pi/\alpha)]^{-\beta/\nu} \tag{3.23}$$

in the wedge, where $\beta/\nu=1/8$ within the Ising universality class considered here. Note that conformal invariance *completely* determines the universal amplitude function $\mathcal{C}(\theta;\alpha)$ [see Eq. (2.10)] as

$$\mathcal{C}(\theta;\alpha)=(\pi/\alpha)^{\beta/\nu}[\sin(\theta\pi/\alpha)]^{-\beta/\nu}, \quad d=2, \tag{3.24}$$

which would remain unspecified by scale invariance considerations alone.

Using Eqs. (3.24) and (3.7) we obtain the relation

$$\frac{r(\theta;\alpha)}{z_0}=\frac{\pi/\alpha}{\sin(\theta\pi/\alpha)}, \quad d=2 \tag{3.25}$$

for the contour lines of the order parameter profile. The deviation Δr from the asymptotic contour lines at the center of the wedge, i.e., $\theta=\alpha/2$, is defined as shown in Fig. 1. We obtain

$$\frac{\Delta r}{z_0}=\frac{\pi}{\alpha}-\frac{1}{\sin(\alpha/2)}, \quad d=2. \tag{3.26}$$

In the limit $\alpha\to\pi$, Eq. (3.26) yields the expansion

$$\frac{\Delta r}{z_0}=\left(1-\frac{\alpha}{\pi}\right)+\left(1-\frac{\pi^2}{8}\right)\left(1-\frac{\alpha}{\pi}\right)^2+O\left(\left(1-\frac{\alpha}{\pi}\right)^3\right), \quad d=2, \tag{3.27}$$

which is the analog of Eq. (3.10) for $d=2$. For $\alpha\to 0$, from Eq. (3.26) we obtain

$$\frac{\Delta r}{z_0}=\frac{\pi-2}{\alpha}+O(\alpha), \quad d=2, \tag{3.28}$$

which is the analog of Eq. (3.11). Note that Eqs. (3.10) and (3.27) and (3.11) and (3.28), respectively, are very similar even in a quantitative sense, i.e., the dependence on the spatial dimension d is weak.

We close this subsection with a discussion of the short-distance expansion of the order parameter according to Eq. (3.12) for the case $d=2$. The thermal average of the stress tensor $\langle T\rangle$ in the wedge can be obtained by means of a conformal mapping from the half-plane [25] and in polar coordinates it reads

$$\langle T_{rr}\rangle=-\langle T_{\theta\theta}\rangle=\frac{c}{24\pi}\left[\left(\frac{\pi}{\alpha}\right)^2-1\right]\frac{1}{r^2}, \tag{3.29a}$$

$$\langle T_{r\theta}\rangle=\langle T_{\theta r}\rangle=0, \tag{3.29b}$$

where c is the conformal anomaly number. The distant-wall correction for the order parameter profile according to Eq. (3.13) can be directly calculated from the expansion of Eq. (3.23) for small θ, with the result

$$M(r,\theta,t=0;\alpha)=M(r,\theta,t=0;\pi)\left\{1+\frac{\beta}{6\nu}\left[\left(\frac{\pi}{\alpha}\right)^2-1\right]\theta^2+O(\theta^4)\right\}. \tag{3.30}$$

From Eqs. (3.12), (3.29), and (3.30) we obtain $b_\phi=-(4\pi/c)\beta/\nu$ in $d=2$. For the Ising universality class considered here ($c=1/2$ and $\beta/\nu=1/8$) we have $b_\phi=-\pi$. Finally, we note that the next-to-leading distant-wall correction $O(\theta^4)$ indicated in Eq. (3.30) stems from $\Delta_r T_{\theta\theta}$ and $(T_{\theta\theta})^2$ because both operators have the same scaling dimension four.

IV. STATIC STRUCTURE FACTOR

The static structure factor $S(|\mathbf{q}|)$ in a bulk system is given by the Fourier transform of the two-point correlation function $G(|\mathbf{r}-\mathbf{r}'|)$, where $\mathbf{q}$ denotes the momentum transfer and $\mathbf{r}$ and $\mathbf{r}'$ are positions in space. Due to translational invariance and isotropy of the bulk the moduli of the momentum transfer and the distance in space remain as the only arguments in Fourier space and real space, respectively. In the wedge geometry translational invariance and isotropy only hold in the $(d-2)$-dimensional subspace along the edge so that the position dependence of G is more complicated. Apart from modifications of the eigenmode spectrum caused by different boundary conditions we follow the derivation of G for a wedge as given in Ref. [20].

A. Mean-field theory

Starting from the formal definition $G(\mathbf{r};\mathbf{r}')\equiv[\delta m(\mathbf{r})/\delta h(\mathbf{r}')]_{h=0}$, where $m(\mathbf{r})$ denotes the order parameter profile and $h(\mathbf{r})$ is an external spatially varying field, we obtain

$$-\Delta G(\mathbf{r};\mathbf{r}')+6m^2(\mathbf{r})G(\mathbf{r};\mathbf{r}')=\delta(\mathbf{r}-\mathbf{r}') \tag{4.1}$$

at the critical point and within mean-field theory. For $\mathbf{r}=(r,\theta,\mathbf{x}_\parallel)$ we apply a Fourier transform with respect to $\mathbf{x}_\parallel$ and define $S(\mathbf{p};r,\theta;r',\theta')$ by [20]

$$G(r,\theta,\mathbf{x}_\parallel;r',\theta',\mathbf{x}_\parallel') = \int \frac{d^{d-2}p}{(2\pi)^{d-2}} S(\mathbf{p};r,\theta;r',\theta')\exp[i\mathbf{p}\cdot(\mathbf{x}_\parallel-\mathbf{x}_\parallel')]. \quad (4.2)$$

From Eqs. (4.1) and (4.2) and by using $m(\mathbf{r})=\mathcal{C}(\theta;\alpha)r^{-1}$ [see Eq. (3.3)], one obtains

$$-\left[\frac{\partial^2}{\partial r^2}+\frac{1}{r}\frac{\partial}{\partial r}+\frac{1}{r^2}\frac{\partial^2}{\partial\theta^2}-p^2\right]S+\frac{6}{r^2}[\mathcal{C}(\theta;\alpha)]^2 S = \frac{1}{r}\delta(r-r')\delta(\theta-\theta'). \quad (4.3)$$

We solve Eq. (4.3) in terms of eigenfunctions to a spectrum E of eigenvalues for the operator on the left-hand side of Eq. (4.3). Each eigenfunction can be written as a product of a radial part $R(r)$ and an angular part $\psi(\theta)$. For the shifted spectrum $\kappa^2=E-\mathbf{p}^2$ the corresponding eigenvalue equations are given by

$$R_n''(r)+r^{-1}R_n'(r)+(\kappa^2-\lambda_n r^{-2})R_n(r)=0 \quad (4.4)$$

and

$$-\psi_n''(\theta)+6[\mathcal{C}(\theta;\alpha)]^2\psi_n(\theta)=\lambda_n\psi_n(\theta), \quad (4.5)$$

where Eq. (4.4) is a Bessel equation with parameter κ and Eq. (4.5) is a Lamé equation. In general the discrete eigenvalues λ_n cannot be given in closed form (see Appendix B for details). Apart from the specific spectrum $\{\lambda_n\}$ and the corresponding eigenfunctions $\{\psi_n\}$ one can represent the solution of Eq. (4.3) in the same form as in Ref. [20], i.e.,

$$S(\mathbf{p};r,\theta;r',\theta') = \frac{2}{\alpha}\sum_{n=3}^{\infty}\int_0^\infty d\kappa\,\kappa\frac{J_{\sqrt{\lambda_n}}(\kappa r)J_{\sqrt{\lambda_n}}(\kappa r')}{\kappa^2+\mathbf{p}^2}\psi_n(\theta)\psi_n(\theta') = \frac{2}{\alpha}\sum_{n=3}^{\infty} I_{\sqrt{\lambda_n}}(pr_<)K_{\sqrt{\lambda_n}}(pr_>)\psi_n(\theta)\psi_n(\theta'), \quad (4.6)$$

where $p=|\mathbf{p}|$, $r_<=\min(r,r')$, and $r_>=\max(r,r')$. In order to determine the decay of the two-point correlation function in real space we insert Eq. (4.6) into Eq. (4.2), and proceed along the lines described in Ref. [20]. The decay of G away from the edge is governed by the critical exponent $\eta_{e\perp}(\alpha)$ according to

$$G(r,\theta,\mathbf{x}_\parallel;r'\to\infty,\theta',\mathbf{x}_\parallel')\sim\frac{1}{(r')^{d-2+\eta_{e\perp}(\alpha)}}, \quad (4.7)$$

and as in Ref. [20] we find from Eq. (4.2) that in the limit $r'/r\to\infty$ the smallest eigenvalue in the spectrum $\{\lambda_n\}$ determines the exponent $\eta_{e\perp}(\alpha)$. With the notation used in Appendix B the smallest eigenvalue is λ_3 and in accordance with Ref. [20], we find $\eta_{e\perp}(\alpha)=\sqrt{\lambda_3}$. Along the edge, i.e., in the limit $|\mathbf{x}_\parallel-\mathbf{x}_\parallel'|\to\infty$ for $r,r'>0$ the decay of G is governed by the critical exponent $\eta_{e\parallel}(\alpha)$ according to

$$G(r,\theta,\mathbf{x}_\parallel;r',\theta',\mathbf{x}_\parallel'\to\infty)\sim\frac{1}{|\mathbf{x}_\parallel-\mathbf{x}_\parallel'|^{d-2+\eta_{e\parallel}(\alpha)}}. \quad (4.8)$$

In agreement with the general scaling relation

$$\eta_{e\perp}(\alpha)=\frac{\eta+\eta_{e\parallel}(\alpha)}{2}, \quad 2\leqslant d\leqslant 4, \quad (4.9)$$

we find $\eta_{e\parallel}(\alpha)=2\eta_{e\perp}(\alpha)$ within mean-field theory (for which $\eta=0$). From the approximate evaluation of the spectrum $\{\lambda_n\}$ [see Eq. (B6) in Appendix B] we obtain

$$\eta_{e\perp}(\alpha)=\sqrt{\lambda_3}\approx\frac{3\pi}{\alpha}\sqrt{1-\frac{4\alpha}{3\pi^2}\zeta(\alpha/2)+\frac{2\alpha^2}{9\pi^4}\left(\pi^2+\frac{g_2(\alpha)}{24}\alpha^2-2\zeta^2(\alpha/2)\right)} \quad (4.10)$$

where $\zeta(u)$ is the Weierstrass ζ function [see Eq. (A9)] and

$$g_2(\alpha)=\frac{4k^2(\alpha)[1-k^2(\alpha)]}{[1-2k^2(\alpha)]^2}+\frac{4}{3} \quad (4.11)$$

[see Eq. (B1)]. In the limit $\alpha\to\pi$ corresponding to a planar surface Eq. (4.10) becomes exact and one obtains $\eta_\perp\equiv\eta_{e\perp}(\pi)=3$ in accordance with the mean-field result for the semi-infinite geometry at the normal transition [18]. The dependence of $\eta_{e\perp}$ on α is displayed in Fig. 5 for $d=2$ [see Eq. (4.16) in Sec. IV B] and 4 [see Eq. (4.10)], where the overall $1/\alpha$ dependence has been split off. The estimate for $d=3$ is obtained by interpolating linearly between the curves for $d=2$ and 4 (compare Figs. 2 and 3). The exponent $\eta_{e\perp}(\alpha)$ increases monotonically as α decreases. This implies that at the normal transition the correlation function decays more rapidly away from an edge ($\alpha<\pi$) than away from a planar surface ($\alpha=\pi$).

Finally, we note that from the general scaling relation for the edge exponent

$$\beta_e(\alpha)=\frac{\nu[d-2+\eta_{e\parallel}(\alpha)]}{2}, \quad 2\leqslant d\leqslant 4, \quad (4.12)$$

which describes the singular temperature dependence of the order parameter at the edge, within mean-field theory one has [see Eq. (4.9), here $\eta=0$ and $\nu=1/2$]

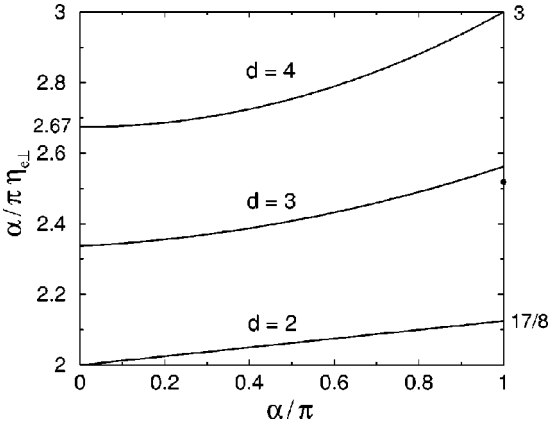

FIG. 5. Universal dependence of the edge exponent $\eta_{e\perp}(\alpha)$ [see Eq. (4.7)] on the opening angle α, with the overall $1/\alpha$ dependence split off. The curve for $d=3$ shows the linear interpolation between the exactly known curves for $d=2$ [see Eq. (4.16)] and $d=4$ [see Eq. (4.10)]. The dot for $\alpha/\pi=1$ shows the known value $\eta_\perp=(\eta+\eta_\parallel)/2\simeq 2.518$ corresponding to a planar surface in $d=3$. The small difference between the dot and the value of the interpolated curve for $d=3$ is a measure of the uncertainty associated with the aforementioned linear interpolation scheme.

$$\beta_e(\alpha)=\frac{1+\eta_{e\perp}(\alpha)}{2},\quad d=4. \tag{4.13}$$

In the limit $\alpha\to\pi$ corresponding to a planar surface Eq. (4.13) yields $\beta_e(\pi)=\beta_1=2$, in accordance with the general scaling relation $\beta_1=d\nu$ for $2\leqslant d\leqslant 4$ at the normal transition for the semi-infinite geometry [36].

B. Exact results in $d=2$

In $d=2$ rigorous results for the edge exponent $\eta_{e\perp}(\alpha)$ can be obtained starting from the correlation function in the half-plane at the normal transition [49]

$$G(x,y;x',y')=(yy')^{-\eta/2}\mathcal{G}\left(\frac{(x-x')^2+y^2+y'^2}{yy'}\right), \tag{4.14}$$

where x and x' are the coordinates of the two points along the surface, and y and y' are their distances from the surface [49]. Applying the conformal mapping and carrying out the limit $r'/r\to\infty$ at fixed $r>0$ leads to

$$G(r,\theta;r',\theta')\sim\left(\frac{\pi}{\alpha}\right)^{\eta}\left[\sin\left(\frac{\pi}{\alpha}\theta\right)\sin\left(\frac{\pi}{\alpha}\theta'\right)\right]^{(\eta_\parallel-\eta)/2}\times(rr')^{-\eta/2}\left(\frac{r'}{r}\right)^{-\pi\eta_\parallel/(2\alpha)} \tag{4.15}$$

for the correlation function in the wedge. From Eq. (4.15) one can read off the scaling relation [49]

$$\eta_{e\perp}(\alpha)=\frac{\eta}{2}+\frac{\pi}{\alpha}\frac{\eta_\parallel}{2}. \tag{4.16}$$

In the limit $\alpha\to\pi$ corresponding to a planar surface one has $\eta_{e\perp}(\pi)=(\eta+\eta_\parallel)/2=\eta_\perp$, as expected [see Eq. (4.9)]. In $d=2$ the edge consists of a single point so that one cannot define correlations along the edge. However, if we formally define $\eta_{e\parallel}(\alpha)$ by Eq. (4.9) we find $\eta_{e\parallel}(\alpha)=(\pi/\alpha)\eta_\parallel$. From $\beta_1=2$ [36] we obtain $\eta_\parallel=4$ at the normal transition within the Ising universality class, which implies [see Eq. (4.12); here $\nu=1$]

$$\beta_e(\alpha)=\frac{\eta_{e\parallel}(\alpha)}{2}=\frac{2\pi}{\alpha},\quad d=2 \tag{4.17}$$

for the edge exponent of the magnetization. We note that β_e given by Eq. (4.17) is four times larger than its corresponding value at the ordinary transition [20–22].

V. SUMMARY

We have investigated the universal local properties of the order parameter profile in a wedge with opening angle α (see Fig. 1) for the normal transition. We have obtained the following main results.

(1) Near T_c the order parameter is determined by universal scaling functions and the two nonuniversal bulk amplitudes a and ξ_0^+ [see Eq. (2.3)]. At T_c the order parameter profile reduces to a power law $r^{-\beta/\nu}$ in radial direction multiplied by a universal amplitude function depending on the polar angle θ and the opening angle α [see Eqs. (2.6) and (2.10)]. The amplitude function is symmetric around the midplane and diverges as $\theta^{-\beta/\nu}$ upon approaching the surfaces forming the wedge [see Eq. (2.13)].

(2) We have determined the universal amplitude function $\mathcal{C}(\theta,\alpha)$ within mean-field theory, i.e., for space dimension $d=4$ [see Eqs. (3.5) and (3.6)], where the order parameter profile in the wedge and for $T=T_c$ can be obtained from the order parameter profile in the film geometry for $T<T_c$ [see Eq. (3.4)]. In conjunction with exact results in $d=2$ [see Eq. (3.24)] we construct an estimate for $\mathcal{C}(\theta,\alpha)$ for $d=3$ (see Fig. 2).

(3) The amplitude function determines the meniscuslike contour lines of a constant value of the critical order parameter profile [see Eq. (3.7) and Fig. 1]. The deviation Δr of the contour line relative to its asymptotes (compare Fig. 1) from the corner of the wedge vanishes linearly in the planar limit $\alpha\to\pi$ [see Eqs. (3.10) and (3.27)] and diverges $\sim\alpha^{-1}$ for $\alpha\to 0$ [see Eqs. (3.11) and (3.28)]. Figure 3 presents an estimate of the function $\Delta r(\alpha)$ for $d=3$.

(4) The contour lines approach their asymptotes as y^{-d} for increasing lateral distance y [see Fig. 1 and Eq. (3.20)]. This follows from an analysis of distant-wall corrections in terms of the stress tensor (see Sec. III C). The explicit results for $d=2$ and 4 allow one to construct an estimate for the corresponding behavior in $d=3$ (see Fig. 4).

(5) The decay of the two-point correlation function at T_c away from the edge and parallel to the wedge is governed by the critical edge exponents $\eta_{e\perp}(\alpha)$ and $\eta_{e\parallel}(\alpha)$, respectively [see Eqs. (4.7) and (4.8)]. They fulfill the scaling relation $\eta_{e\perp}(\alpha)=[\eta+\eta_{e\parallel}(\alpha)]/2$ with the bulk exponent η. Based on the quite accurate estimate in $d=4$ [see Eq. (4.10) and Appendix B] and the exact result in $d=2$ [see Eq. (4.16)] Figure 5 presents an estimate for $\eta_{e\perp}(\alpha)$ in $d=3$. Equations (4.13) and (4.17) provide the critical edge exponent $\beta_e(\alpha)$ of the order parameter for the normal transition. Equation (4.6)

gives the full structure factor for the wedge geometry and for $T=T_c$ within the mean-field approximation.

ACKNOWLEDGMENTS

We thank G. Sommer for helpful collaboration at an early stage of this work. M.K. gratefully acknowledges support by the German Science Foundation through a Heisenberg Stipendium. The work of A.H. and S.D. was supported by the German Science Foundation through Sonderforschungsbereich 237.

APPENDIX A: ELLIPTIC FUNCTIONS

Here we summarize a few properties of elliptic functions as far as they are needed for the derivation of the results obtained in this paper. For further information we refer to the literature (see, e.g., Refs. [50–52]). The properties of the Jacobian elliptic functions can be derived starting from the Jacobi amplitude $\mathrm{am}(u;k)$ which is implicitly defined by the incomplete elliptic integral of the first kind:

$$u=\int_0^{\mathrm{am}(u;k)}\frac{d\varphi}{\sqrt{1-k^2\sin^2\varphi}}. \tag{A1}$$

The complete elliptic integral of the first kind $K=K(k)$ is defined by $\mathrm{am}(K;k)=\pi/2$. For the derivation of Eq. (3.10) we quote the expansion of $K(k)$ in powers of the modulus k:

$$K(k)=\frac{\pi}{2}\left[1+\frac{1}{4}k^2+\frac{9}{64}k^4+O(k^6)\right]. \tag{A2}$$

From the first derivative of Eq. (A1) with respect to u, for $k^2\leqslant 1$ one obtains the relation

$$\mathrm{dn}(u;k)\equiv\frac{\partial}{\partial u}\mathrm{am}(u;k)=\sqrt{1-k^2\,\mathrm{sn}^2(u;k)} \tag{A3}$$

for the delta amplitude $\mathrm{dn}(u;k)$ using the standard notations

$$\mathrm{sn}(u;k)\equiv\sin[\mathrm{am}(u;k)],\quad \mathrm{cn}(u;k)\equiv\cos[\mathrm{am}(u;k)]. \tag{A4}$$

Due to $\mathrm{am}(0;k)=0$ and $\mathrm{am}(K;k)=\pi/2$, one has

$$\mathrm{sn}(0;k)=0,\quad \mathrm{cn}(0;k)=1,\quad \mathrm{dn}(0;k)=1, \tag{A5a}$$

$$\mathrm{sn}(K;k)=1,\quad \mathrm{cn}(K;k)=0,\quad \mathrm{dn}(K;k)=\sqrt{1-k^2}. \tag{A5b}$$

The derivation of Eq. (3.17) is based on the Taylor expansions

$$\mathrm{sn}(u;k)=u-\frac{1+k^2}{3!}u^3+\frac{1+14k^2+k^4}{5!}u^5-\frac{1+135k^2+135k^4+k^6}{7!}u^7+O(u^9), \tag{A6a}$$

$$\mathrm{dn}(u;k)=1-\frac{k^2}{2}u^2+\frac{k^2(4+k^2)}{4!}u^4-\frac{k^2(16+44k^2+k^4)}{6!}u^6+O(u^8). \tag{A6b}$$

Finally, we quote the relation

$$E(\mathrm{am}(u;k),k)=\int_0^u \mathrm{dn}^2(x;k)\,dx=\int_0^{\mathrm{am}(u;k)}\sqrt{1-k^2\sin^2\varphi}\,d\varphi \tag{A7}$$

between the incomplete elliptic integral of the second kind $E(x,k)$ and the delta amplitude $\mathrm{dn}(u;k)$. $E(k)\equiv E(\pi/2,k)$ is the complete elliptic integral of the second kind.

As demonstrated in Appendix A of Ref. [41] the mean-field order parameter profile can be obtained from the observation that $[\mathcal{C}(\theta;\alpha)]^2$ is a Weierstrass $\wp$ function up to an additive constant. The Weierstrass $\wp$ function is an elliptic function which is related to squares of certain Jacobian elliptic functions [50,51]. It solves the differential equation

$$[\wp'(u)]^2=4\wp^3(u)-g_2\wp(u)-g_3, \tag{A8}$$

where g_2 and g_3 are the invariants of $\wp$. Note that no term quadratic in $\wp$ appears on the right-hand side of Eq. (A8). This condition determines the additive constant in the relation between $\wp$ and $\mathcal{C}^2$ which appears as the ''potential'' in the eigenvalue problem in Eq. (4.5). For the derivation of the spectrum $\{\lambda_n\}$ (see Appendix B) the Weierstrass ζ function is also needed. It is the negative integral of $\wp(u)$ and can be written as

$$\zeta(u)=\frac{1}{u}-\int_0^u\left[\wp(z)-\frac{1}{z^2}\right]dz. \tag{A9}$$

Note that $\zeta(u)$ is *not* an elliptic function. For the explicit calculation of the spectrum $\{\lambda_n\}$ we finally quote the Laurent series of $\wp(u)$ and $\zeta(u)$ around $u=0$:

$$\zeta(u)=\frac{1}{u}-\frac{g_2}{60}u^3-\frac{g_3}{140}u^5+O(u^7), \tag{A10a}$$

$$\wp(u)=\frac{1}{u^2}+\frac{g_2}{20}u^2+\frac{g_3}{28}u^4+O(u^6). \tag{A10b}$$

APPENDIX B: EIGENMODE SPECTRUM

The spectrum of the eigenvalue problem defined by Eq. (4.5) can be determined along similar lines as in Appendix B of Ref. [41]. The Weierstrass function associated with $\mathcal{C}(\theta;\alpha)$ [see Eq. (3.5)] can be written in the form $\wp(\theta)=\mathcal{C}^2(\theta;\alpha)-a$, where a is a constant to be determined. Based on Eq. (3.4) we aim at obtaining a differential equation for $\wp$ which is of the form given by Eq. (A8). This requirement is fulfilled if $a=1/3$, which results in

$$\wp(\theta)=\left[\frac{2K}{\alpha}\frac{\mathrm{dn}(2K\theta/\alpha;k)}{\mathrm{sn}(2K\theta/\alpha;k)}\right]^2-\frac{1}{3}, \tag{B1a}$$

$$g_2=\frac{4k^2(1-k^2)}{(1-2k^2)^2}+\frac{4}{3}, \tag{B1b}$$

$$g_3=\frac{4k^2(1-k^2)}{3(1-2k^2)^2}+\frac{8}{27}. \tag{B1c}$$

The eigenvalue problem in Eq. (4.5) can now be cast into a Lamé equation [52]

$$-\psi_n''(\theta)+6\wp(\theta)\psi_n(\theta)=\epsilon_n\psi_n(\theta), \tag{B2}$$

where $\epsilon_n=\lambda_n-2$. As discussed in Appendix B in Ref. [41], the eigenvalue spectrum is given by the solution of the two equations

$$2a_n\zeta(\alpha/2)-\alpha\left[\zeta(a_n)+\frac{\wp'(a_n)}{2\wp(a_n)-\epsilon_n/3}\right]=n\pi i, \tag{B3a}$$

$$\wp(a_n)=\frac{\epsilon_n^3-27g_3}{27g_2-9\epsilon_n^2}. \tag{B3b}$$

The mode numbers n are integers (see below) and a_n are auxiliary parameters with the property $a_n\to 0$ for $n\to\infty$. For large n, Eq. (B3) can be solved asymptotically by using the expansions quoted in Eq. (A10). From the expansion for $\wp(a_n)$ for large n we obtain

$$\epsilon_n=-\frac{9}{a_n^2}\left[1+\frac{7g_2}{540}a_n^4+O(a_n^6)\right], \tag{B4}$$

which implies the expansion

$$\frac{2}{\alpha}\zeta(\alpha/2)a_n-\frac{3}{a_n}-\frac{g_2}{180}a_n^3+O(a_n^5)=\frac{n\pi i}{\alpha}. \tag{B5}$$

Equation (B5) can be solved with the ansatz $a_n=3\alpha i/(n\pi)[1+An^{-2}+Bn^{-4}+O(n^{-6})]$. Inserting the solution into Eq. (B4) leads to

$$\epsilon_n=\left(\frac{n\pi}{\alpha}\right)^2\left\{1-\frac{12}{(n\pi)^2}\alpha\zeta(\alpha/2)-\frac{36}{(n\pi)^4}\left[(\alpha\zeta(\alpha/2))^2-\frac{g_2}{48}\alpha^4\right]+O(n^{-6})\right\}; \tag{B6}$$

$\lambda_n=\epsilon_n+2$ yields the desired spectrum.

The allowed mode numbers n can be obtained by considering the special case $\alpha=\pi$ corresponding to a planar surface, for which $\mathcal{C}(\theta;\pi)=1/\sin\theta$ and Eq. (4.5) can be solved in closed form. For the present problem the Weierstrass ζ function can directly be derived from Eqs. (A9) and (B1), so that

$$\zeta(\theta)=\frac{2K}{\alpha}\left[\frac{\mathrm{dn}(2K\theta/\alpha;k)}{\mathrm{sn}(2K\theta/\alpha;k)}\mathrm{cn}(2K\theta/\alpha;k)+E(\mathrm{am}(2K\theta/\alpha;k),k)+\frac{k^2-2}{3}\frac{2K}{\alpha}\theta\right], \tag{B7}$$

with $K=K(k)$ as defined in Appendix A. Equation (B7) explicitly demonstrates that $\zeta(\theta)$ is not an elliptic function. At the midplane $\theta=\alpha/2$, Eq. (B7) reduces to [see Eq. (A5)]

$$\zeta(\alpha/2)=\frac{2K(k)}{\alpha}\left[E(k)+\frac{k^2-2}{3}K(k)\right]. \tag{B8}$$

According to Eq. (3.5b) the special case $\alpha=\pi$ corresponds to $k=0$ for which $\zeta(\pi/2)=\pi/6$ from Eq. (B8) and $g_2=4/3$ from Eq. (B1). From Eq. (B6) we infer that $\epsilon_n=n^2-2$, i.e., $\lambda_n=n^2$, which is indeed the correct eigenvalue spectrum for $\mathcal{C}(\theta;\pi)=1/\sin\theta$. The eigenfunctions are normalizable for $n\geqslant 3$. Therefore, λ_3 is the lowest eigenvalue for this problem.

For a numerical solution of Eq. (B3) using, e.g., the Newton method the asymptotic spectrum given by Eq. (B6) for $n\geqslant 3$ provides excellent initial values for the iteration. In fact, these initial values already are within 0.1% of the exact spectrum even for the ground state $n=3$ if $0.1<\alpha/\pi\leqslant 1$. This implies that the mean-field expression for $\eta_{e\perp}(\alpha)$ given by Eq. (4.10) is quite accurate if α is not too small.

[1] W. Hansen, J. P. Kotthaus, and U. Merkt, in *Nonstructured Systems*, edited by M. Reed, Semiconductors and Semimetals Vol. 35 (Academic, London, 1992), p. 279; see also P. Bönsch, D. Wüllner, T. Schrimpf, A. Schlachetski, and R. Lacmann, J. Electrochem. Soc. **145**, 1273 (1998); J. Wang, D. A. Thompson, and J. G. Simmons, *ibid.* **145**, 2931 (1998).

[2] D. W. L. Tolfree, Rep. Prog. Phys. **61**, 313 (1998).

[3] Y. Xia and G. M. Whitesides, Annu. Rev. Mater. Sci. **28**, 153 (1998).

[4] F. Burmeister, C. Schäfle, B. Keilhofer, C. Bechinger, J. Boneberg, and P. Leiderer, Adv. Mater. **10**, 495 (1998).

[5] J. B. Knight, A. Vishwanath, J. P. Brody, and R. H. Austin, Phys. Rev. Lett. **80**, 3863 (1998).

[6] M. Grunze, Science **283**, 41 (1999).

[7] R. F. Service, Science **282**, 399 (1998).

[8] S. Dietrich, in *New Approaches to Old and New Problems in Liquid State Theory: Inhomogeneities and Phase Separation in Simple, Complex and Quantum Fluids*, Vol. 529 of *NATO Advanced Study Institute Series C: Mathematical and Physical Sciences*, edited by C. Caccamo, J. P. Hansen, and G. Stell (Kluwer, Dordrecht, 1999), p. 197.

[9] M. Schoen and S. Dietrich, Phys. Rev. E **56**, 499 (1997).

[10] D. Henderson, S. Sokołowski, and D. Wasan, Phys. Rev. E **57**, 5539 (1998).

[11] A. J. P. Nijmeijer and J. N. J. van Leeuwen, J. Phys. A **23**, 4211 (1990).

[12] M. Napiórkowski, W. Koch, and S. Dietrich, Phys. Rev. A **45**, 5760 (1992).

[13] E. H. Hauge, Phys. Rev. A **46**, 4994 (1992).

[14] A. Lipowski, Phys. Rev. E **58**, R1 (1998).

[15] K. Rejmer, S. Dietrich, and M. Napiórkowski, Phys. Rev. E **60**, 4027 (1999), and references therein.

[16] P. Müller-Buschbaum, M. Tolan, W. Press, F. Brinkop, and J. P. Kotthaus, Ber. Bunsenges. Phys. Chem. **98**, 413 (1994).

[17] Z. Li, M. Tolan, T. Höhr, D. Kharas, S. Qu, J. Sokolov, M. H.

Rafailovich, H. Lorenz, J. P. Kotthaus, J. Wang, S. K. Sinha, and A. Gibaud, Macromolecules **31**, 1915 (1998).
[18] K. Binder, in *Phase Transitions and Critical Phenomena*, edited by C. Domb and J. L. Lebowitz (Academic, London, 1983), Vol. 8, p. 1.
[19] H. W. Diehl, in *Phase Transitions and Critical Phenomena*, edited by C. Domb and J. L. Lebowitz (Academic, London, 1986), Vol. 10, p. 75; H. W. Diehl, Int. J. Mod. Phys. B **11**, 3503 (1997).
[20] J. L. Cardy, J. Phys. A **16**, 3617 (1983).
[21] A. J. Guttmann and G. M. Torrie, J. Phys. A **17**, 3539 (1984).
[22] M. N. Barber, I. Peschel, and P. A. Pearce, J. Stat. Phys. **37**, 497 (1984); I. Peschel, Phys. Lett. A **110**, 313 (1985).
[23] T. A. Larsson, J. Phys. A **19**, 1691 (1986).
[24] D. B. Abraham and F. T. Latrémolière, J. Stat. Phys. **81**, 539 (1995); Phys. Rev. Lett. **76**, 4813 (1996); Nucl. Phys. B **45A**, 74 (1996).
[25] P. Kleban and I. Peschel, Z. Phys. B **101**, 447 (1996).
[26] B. Davies and I. Peschel, Ann. Phys. (N.Y.) **6**, 187 (1997).
[27] D. Karevski, P. Lajkó, and L. Turban, J. Stat. Phys. **86**, 1153 (1997).
[28] M. Pleimling and W. Selke, Eur. Phys. J. B **5**, 805 (1998).
[29] M. Pleimling and W. Selke, Phys. Rev. B **59**, 65 (1999).
[30] I. Peschel, L. Turban, and F. Iglói, J. Phys. A **24**, L1229 (1991).
[31] F. Iglói, I. Peschel, and L. Turban, Adv. Phys. **42**, 683 (1993).
[32] C. Kaiser and L. Turban, J. Phys. A **28**, 351 (1995).
[33] J. Unguris, R. J. Celotta, and D. T. Pierce, Phys. Rev. Lett. **67**, 140 (1991); **69**, 1125 (1992).
[34] A. Ciach and H. W. Diehl, Europhys. Lett. **12**, 635 (1990); H. W. Diehl and A. Ciach, Phys. Rev. B **44**, 6642 (1991).
[35] H. W. Diehl and M. Smock, Phys. Rev. B **47**, 5841 (1993); **48**, 6740 (1993).
[36] H. W. Diehl, Ber. Bunsenges. Phys. Chem. **98**, 466 (1994); Phys. Rev. B **49**, 2846 (1994); T. W. Burkhardt and H. W. Diehl, Phys. Rev. B **50**, 3894 (1994).
[37] G. Flöter and S. Dietrich, Z. Phys. B **97**, 213 (1995).
[38] D. S. P. Smith and B. M. Law, Phys. Rev. E **52**, 580 (1995); **54**, 2727 (1996); **55**, 620 (1997).
[39] P. S. Swain and A. O. Parry, Eur. Phys. J. B **4**, 459 (1998); C. Rascón and A. O. Parry, Phys. Rev. Lett. **81**, 1267 (1998); C. Rascón, A. O. Parry, and A. Sartori, Phys. Rev. E **59**, 5697 (1999).
[40] J. C. Le Guillou and J. Zinn-Justin, J. Phys. (France) Lett. **46**, L137 (1985); R. Guida and J. Zinn-Justin, J. Phys. A **31**, 8103 (1998).
[41] M. Krech, Phys. Rev. E **56**, 1692 (1997).
[42] M. E. Fisher and H. Au-Yang, Physica A **101**, 255 (1980).
[43] J. Rudnick and D. Jasnow, Phys. Rev. Lett. **49**, 1595 (1982).
[44] J. L. Cardy, in *Phase Transitions and Critical Phenomena*, edited by C. Domb and J. L. Lebowitz (Academic, London, 1986), Vol. 11, p. 55.
[45] J. L. Cardy, Phys. Rev. Lett. **65**, 1443 (1990).
[46] E. Eisenriegler and M. Stapper, Phys. Rev. B **50**, 10 009 (1994).
[47] M. E. Fisher and P. G. de Gennes, C. R. Seances Acad. Sci., Ser. B **287**, 207 (1978).
[48] T. W. Burkhardt and E. Eisenriegler, J. Phys. A **18**, L83 (1985).
[49] J. L. Cardy, Nucl. Phys. B **240**, 514 (1984).
[50] D. F. Lawden, *Elliptic Functions and Applications* (Springer, New York, 1989).
[51] M. Abramowitz and I. A. Stegun, *Handbook of Mathematical Functions* (Dover, New York, 1972); I. S. Gradshteyn and I. M. Ryzhik, *Table of Integrals, Series, and Products* (Academic, London, 1965).
[52] E. Kamke, *Differentialgleichungen, Lösungsmethoden und Lösungen* (Chelsea, New York, 1971), Vol. 1, p. 408.